

## RESEARCH ARTICLE

# Zinc and manganese homeostasis closely interact in mammalian cells

Yukina Nishito<sup>1</sup> | Yoshiki Kamimura<sup>1</sup> | Shino Nagamatsu<sup>1</sup> | Nao Yamamoto<sup>1</sup> |  
Hiroyuki Yasui<sup>2</sup>  | Taiho Kambe<sup>1</sup> 

<sup>1</sup>Division of Integrated Life Science, Graduate School of Biostudies, Kyoto University, Kyoto, Japan

<sup>2</sup>Department of Analytical and Bioinorganic Chemistry, Division of Analytical and Physical Sciences, Kyoto Pharmaceutical University, Kyoto, Japan

**Correspondence**

Taiho Kambe, Division of Integrated Life Science, Graduate School of Biostudies, Kyoto University, Kyoto 606-8502, Japan.

Email: [kambe.taiho.7z@kyoto-u.ac.jp](mailto:kambe.taiho.7z@kyoto-u.ac.jp)

**Funding information**

Ministry of Education, Culture, Sports, Science and Technology (MEXT), Grant/Award Number: JP19H05768; MEXT | Japan Society for the Promotion of Science (JSPS), Grant/Award Number: JP19H02883, JP22H02257 and JP21K15262; Kieikai Research Foundation; Tojuro Iijima Foundation for Food Science and Technology; Sugiyama Chemical & Industrial Laboratory; KOSE Cosmetology Research Foundation; Naito Foundation

**Abstract**

Understanding the homeostatic interactions among essential trace metals is important for explaining their roles in cellular systems. Recent studies in vertebrates suggest that cellular Mn metabolism is related to Zn metabolism in multifarious cellular processes. However, the underlying mechanism remains unclear. In this study, we examined the changes in the expression of proteins involved in cellular Zn and/or Mn homeostatic control and measured the Mn as well as Zn contents and Zn enzyme activities to elucidate the effects of Mn and Zn homeostasis on each other. Mn treatment decreased the expression of the Zn homeostatic proteins metallothionein (MT) and ZNT1 and reduced Zn enzyme activities, which were attributed to the decreased Zn content. Moreover, loss of Mn efflux transport protein decreased MT and ZNT1 expression and Zn enzyme activity without changing extracellular Mn content. This reduction was not observed when supplementing with the same Cu concentrations and in cells lacking Cu efflux proteins. Furthermore, cellular Zn homeostasis was oppositely regulated in cells expressing Zn and Mn importer ZIP8, depending on whether Zn or Mn concentration was elevated in the extracellular milieu. Our results provide novel insights into the intricate interactions between Mn and Zn homeostasis in mammalian cells and facilitate our understanding of the physiopathology of Mn, which may lead to the development of treatment strategies for Mn-related diseases in the future.

**KEYWORDS**

competition, copper, homeostasis, manganese, metallothionein, TMEM165, transporter, zinc, ZNT1

## 1 | INTRODUCTION

Essential trace elements play crucial roles in a variety of physiological functions, and their deficiency induces

a wide spectrum of clinical disorders, whereas their excessive ingestion can cause toxicity.<sup>1-7</sup> Some of these elements are associated with one another in systemic and cellular homeostasis, and unintended imbalance in their

This is an open access article under the terms of the [Creative Commons Attribution](https://creativecommons.org/licenses/by/4.0/) License, which permits use, distribution and reproduction in any medium, provided the original work is properly cited.

© 2024 The Authors. *The FASEB Journal* published by Wiley Periodicals LLC on behalf of Federation of American Societies for Experimental Biology.

concentrations might be pathological.<sup>8–12</sup> For example, excess Zn causes Cu deficiency, leading to reduction in Fe absorption, eventually resulting in anemia.<sup>9,10</sup> This is because Zn and Cu compete during absorption, and Cu is required for Fe absorption and metabolism.<sup>11</sup> Moreover, Mn toxicity is reported to be associated with Fe deficiency<sup>12,13</sup> because Mn homeostasis partly overlaps with Fe homeostasis; DMT1, ferroportin, and transferrin bind to Mn in addition to Fe.<sup>14,15</sup> Progress in identifying proteins such as transporters, binding proteins, chaperones, and sensor proteins, which are involved in systemic and cellular homeostasis of these metals, raises the possibility that another unique interaction may occur among them. Therefore, the interaction between these metals requires further investigation.

Recently, significant progress was made in understanding the homeostatic control of Mn.<sup>16–18</sup> Mn homeostasis is regulated by secretory pathway Ca-ATPase 1 (SPCA1), which functions as a Ca channel; SPCA1 is responsible for transporting Mn into the Golgi apparatus, playing a vital role in Mn efflux.<sup>19,20</sup> Proteins involved in Fe metabolism, including DMT1, transferrin, and ferroportin, also play important roles in Mn transport, the former two of which are involved in Mn import and the latter is involved in Mn export.<sup>21</sup> Moreover, several Zn importers/exporters are involved in Mn homeostasis, including Zrt/Irt-like protein 14 (ZIP14) and Zn transporter 10 (ZNT10), which play a role in Mn transport<sup>22,23</sup> as identified through analysis of mutations of *ZIP14/SLC39A14* and *ZNT10/SLC30A10* that cause Parkinsonism and dystonia with hypermanganesemia.<sup>24–26</sup> Moreover, *ZIP8/SLC39A8* mutations result in type II congenital disorders of glycosylation (CDG) due to systemic Mn deficiency.<sup>27,28</sup> These findings suggest that cellular Mn homeostasis may be related to Zn homeostasis, although biochemical analysis is lacking. In contrast, the interplay between Zn and Cu is widely investigated in mammals, including humans.<sup>10,29</sup>

Several proteins have been shown to be relevant in investigating the interplay between trace elements. To assess Zn levels, two Zn homeostatic proteins, the cytosolic zinc-binding protein metallothionein (MT) and Zn transporter 1 (ZNT1), are relevant as their expression increases in response to high zinc and decreases during Zn deficiency owing to transcriptional and posttranslational controls.<sup>30–34</sup> In human cells, cellular Zn homeostasis is maintained by 14 members of ZIPs, 10 members of ZNTs, and 11 isoforms of MTs.<sup>35–39</sup> Only MT and ZNT1 ubiquitously show the expression response pattern that allows cells to maintain cytosolic Zn levels within physiological range through mitigating increases in cytosolic Zn concentrations<sup>30–34,40</sup> (in this study, the term “MT” is used to refer to all eight isoforms of MT1s and MT2, as MT3 and MT4 expression does not change in response to Zn

levels<sup>39</sup>). Additionally, some Zn-dependent enzymes are useful to assess the cellular Zn levels because their activities sensitively decrease in response to Zn deficiency. These enzymes are tissue-nonspecific alkaline phosphatase (TNAP), ecto-5'-nucleotidase (NT5E, also known as CD73), ectonucleotide pyrophosphatase/phosphodiesterase 1 (ENPP1), and ENPP3.<sup>41–43</sup> As the homeostatic control of Mn is well understood, the cellular Mn levels have also been assessed using several proteins. One of them is TMEM165, a Golgi membrane protein involved in Mn homeostasis, whose deficiency causes a CDG. Expression of TMEM165 decreases in response to high Mn content following degradation in the lysosomes.<sup>44,45</sup>

In this study, we assume that if Mn affects Zn homeostasis under pathophysiological conditions, Mn treatment would alter MT and ZNT1 expression. To investigate this possibility, we performed a series of experiments that examined MT, ZNT1, and TMEM165 expression as well as Zn enzyme activity, along with measuring Mn and Zn contents, which were compared with those of Cu. We also examined the effect of Mn on Zn homeostasis using genetically engineered cells lacking Mn or Cu efflux proteins. Furthermore, we examined how the expression of ZIP8, a transporter of Zn and Mn, affected cellular Zn and Mn homeostasis when Zn or Mn was elevated in the extracellular milieu. Mn can be beneficial or harmful depending on its concentration in the body.<sup>4–7</sup> Therefore, clarifying its metabolism in cells is important. Our results provide crucial insights into understanding Mn metabolism in mammalian cells.

## 2 | MATERIALS AND METHODS

### 2.1 | Cell culture

Human near-haploid HAP1 cells (Horizon, Discovery, Tokyo, Japan) were maintained at 37°C in a humidified 5% CO<sub>2</sub> incubator in Iscove's modified Dulbecco's medium (Nacalai Tesque, Kyoto, Japan) containing 10% (v/v) heat-inactivated fetal calf serum (FCS) (Biosera, Kansas City, MO, USA), 100 U/mL penicillin, and 100 µg/mL streptomycin (Nacalai Tesque).<sup>42</sup> Dulbecco's modified Eagle's medium (DMEM) (FUJIFILM Wako Pure Chemical Corporation, Osaka, Japan) and RPMI1640 (Nacalai Tesque) were used to maintain HepG2 and FLP-In™ T-Rex Madin–Darby canine kidney (MDCK) cells and PANC1 cells.<sup>32,43</sup> The indicated MnSO<sub>4</sub> or ZnSO<sub>4</sub> concentrations (Nacalai Tesque) were added to the cell culture medium for Mn or Zn treatment, respectively. Zinc-deficient medium (termed CX in this study) was generated using Chelex-100 (CX) resin (Bio-Rad, Hercules, CA, USA)-treated FCS as described previously.<sup>46</sup>

## 2.2 | Plasmid construction

ZIP8 cDNA was PCR amplified using total RNA prepared from A549 cells using Sepasol-RNA I Super G (Nacalai Tesque) as a template. Mouse *Zip14* cDNA was purchased from OriGene (OriGene Technologies, Inc., Rockville, MD, USA). Each cDNA was fused with a sequence encoding an HA epitope tag at the carboxy terminus via a two-step PCR and inserted into the pcDNA5/FRT/TO plasmid (Thermo Fisher Scientific, Waltham, MA, USA).

## 2.3 | Stable transfection

ZIP8 and *Zip14* cDNAs inserted into the pcDNA5/FRT/TO plasmid were transfected in MDCK cells together with the pOG44 plasmid at a 1:1 ratio using Lipofectamine 2000 (Thermo Fisher Scientific) to establish stable transfectants. Stable clones were selected in a medium containing 100–500 µg/mL hygromycin B (Nacalai Tesque) after 3 weeks. MDCK cells stably expressing ZIP5 were previously established.<sup>47</sup> HAP1 cells stably expressing ZNT1 or ZNT10 were generated by transfecting pcDNA3-harboring *ZNT1* or *ZNT10* cDNA using Lipofectamine 2000. Each cDNA was fused with an HA-tag at the carboxy terminus. After transfection, the cells were cultured in the presence of 500–1500 µg/mL G418 (Nacalai Tesque) to select the cells stably transfected with pcDNA3 plasmid containing the neomycin resistance gene.

## 2.4 | Disruption of SPCA1, ATP7A, ATP7B, and ZNT1

The established clones are listed in Table S1. CRISPR/Cas9-mediated genome editing using sgRNA expression plasmids was performed as previously described.<sup>32,48</sup> Oligonucleotides used to generate the sgRNA expression plasmid for the *SPCA1* and *ATP7B* genes<sup>49</sup> are listed in Table S2. The constructed plasmids (4 µg) and one-tenth of the pcDNA6/TR plasmid containing the blasticidin S resistance, or the pcDNA3 plasmid containing the neomycin resistance was co-transfected into 80% confluent HAP1 cells using 4 µL Lipofectamine 2000 and cultured for 1 day. HAP1 cells were transferred onto a 10 cm cell culture dish and cultured in the presence of 15–20 µg/mL blasticidin S (InvivoGen, San Diego, CA, USA) or 500–1500 µg/mL G418 (Nacalai Tesque) for 3 weeks. Genome editing using CRISPR/Cas9 was confirmed by sequencing the genomic DNA-amplified PCR fragments using the primers listed in Table S3. Oligonucleotides for generating

the sgRNA expression plasmid for *ZNT1* or *ATP7A* genes were previously described.<sup>32,48</sup>

## 2.5 | Immunoblotting

Immunoblotting was performed as previously described.<sup>32,47</sup> Cells were lysed in ALP buffer (10 mM Tris-HCl [pH 7.5], 0.5 mM MgCl<sub>2</sub>, and 0.1% TritonX-100 (FUJIFILM Wako Pure Chemical Corporation)). Next, 10–30 µg of total protein or membrane protein was denatured in 6× sodium dodecyl sulfate (SDS) sample buffer at room temperature (25–30°C) for 30 min, separated by electrophoresis on an 8% SDS polyacrylamide gel, and transferred onto polyvinylidene difluoride (PVDF) membranes (Immobilon-P; Millipore Corp., Bedford, MA, USA). To detect MT, total cellular protein lysed in 6× SDS sample buffer was treated as follows before electrophoresis. Proteins were denatured at 95°C for 3 min and mixed with one-ninth volume of 1 M iodoacetamide (final concentration, 100 mM) in the dark for 30 min at room temperature for carboxymethylation of the cysteine residues in MT. Iodoacetamide was quenched by adding 1.5 M Tris-HCl (pH 8.8) at the same volume as that used for 1 M iodoacetamide, followed by incubation for 3 min at room temperature in the dark. Samples were separated by electrophoresis on a 15% SDS-polyacrylamide gel and transferred onto PVDF membranes, which were fixed with 2.5% glutaraldehyde solution for 30 min at room temperature. Membranes were washed twice with distilled water, then washed thrice with distilled water while shaking for 5 min each time, followed by washing once (including shaking) with 0.1% Tween 20 in PBS (PBS-T) for 5 min. Blotted PVDF membranes were blocked with 5% skim milk in PBS-T and incubated with the following primary antibodies (diluted in blocking buffer): anti-HA [HA-11] (1:3000; BioLegend, San Diego, CA), anti-HA [561] (1:3000; MBL, Nagoya, Japan), anti-MT [1A12] (1:3000; TransGenic Inc., Kobe, Japan), anti-ZNT1 (1:3000),<sup>31</sup> anti-TMEM165 [HPA038299] (1:3000; Sigma-Aldrich, St. Louis, USA), anti-TNAP (F4) [sc166261] (1:3000; Santa Cruz Biochemistry), anti-ENPP1 [NBP2-27561] (1:3000; Novus Biologicals, Littleton, CO), anti-ENPP3 [HPA043772] (1:3000; HPA043772; Sigma-Aldrich), anti-NT5E/CD73 [13160] (1:3000; Cell Signaling Technology, Beverly, MA), anti-α-tubulin [12G10] (1:3000; deposited in the Developmental Studies Hybridoma Bank (DSHB) by J. Frankel and E. M. Nelsen), and anti-calnexin [10427-2-AP] (1:3000; Proteintech Group Inc., Chicago, IL). Immunoreactive bands were detected using horseradish peroxidase (HRP)-conjugated anti-mouse or anti-rabbit secondary antibodies (1:3000; NA931 or

NA934; GE Healthcare, Milwaukee, WI, USA) and Immobilon Western Chemiluminescent HRP Substrate (Millipore) according to the manufacturer's instructions. Chemiluminescence images were obtained using an ImageQuant LAS 500 System (Cytiva, Marlborough, MA, USA), and densitometric quantification of band intensity was performed using ImageQuant TL software (Cytiva).

## 2.6 | Immunofluorescence staining

Immunostaining was performed as previously described.<sup>32</sup> Cells were cultured on a coverslip and fixed with 10% formaldehyde-neutral buffer solution (Nacalai Tesque). Coverslips coated with 0.01% poly-L-lysine (Sigma-Aldrich) solution were used for HepG2 cells. After blocking with 6% BSA in PBS, the samples were stained with anti-ZNT1 (1:3000) without permeabilization and subsequently stained with Alexa 594-conjugated goat anti-mouse IgG (Thermo Fisher Scientific) and Alexa 594-conjugated anti-goat rabbit IgG (Thermo Fisher Scientific) as the secondary and tertiary antibodies, respectively. The antibodies were applied at room temperature for 1 h or at 4°C overnight, and 4,6-diamino-2-phenylindole (DAPI; 1:1000; Abcam, Cambridge, UK) was added during secondary antibody staining to label the nuclei. The dilution buffer was BSA (2%) in PBS. Stained cells were examined under a fluorescence microscope (FSX100; Olympus, Tokyo, Japan). Identical exposure settings and times were used for the corresponding images shown in each figure.

## 2.7 | Cytotoxicity assay against high-concentration Mn or Cu

Cell viability was determined using Alamar Blue (Bio-Rad, Hercules, CA, USA) as previously described.<sup>32</sup> HAP1, HepG2, and PANC1 cells were cultured at a density of  $1.0 \times 10^4$  cells/mL in a 96-well plate and treated with the indicated concentrations of  $\text{MnSO}_4$  or  $\text{CuSO}_4$  for 24 h. The Alamar Blue reagent was added to the medium, which was subsequently incubated for 4 h. Absorbance was measured at 570 and 600 nm using a Synergy H1 Hybrid multi-mode microplate reader (BioTek, Winooski, VT, USA).

## 2.8 | Reverse transcription PCR

Total RNA was isolated from harvested HAP1 cells using Sepasol I (Nacalai Tesque) and reverse transcribed using

ReverTra Ace (Toyobo, Osaka, Japan). PCR was performed using KOD-FX (Toyobo) and the primers listed in Table S4. A full-length gel image is provided in Figure S11.

## 2.9 | Measurement of TNAP activity

Cell membrane protein extracts were prepared using ALP lysis buffer (10 mM Tris-HCl, 0.5 mM  $\text{MgCl}_2$ , and 0.1% Triton X-100 at pH 7.5); 3  $\mu\text{g}$  of membrane protein was used to measure TNAP activity, as previously described.<sup>42,43</sup> Lysates were preincubated for 10 min at room temperature, followed by the addition of 100  $\mu\text{L}$  substrate solution [2 mg/mL disodium *p*-nitrophenyl phosphate hexahydrate (*p*NPP; FUJIFILM) in 1 M diethanolamine buffer (pH 9.8) containing 0.5 mM  $\text{MgCl}_2$ ]. The released *p*-nitrophenol product was quantified at 405 nm using a Synergy H1 Hybrid multi-mode microplate reader (BioTek). Calf intestinal ALP (Promega, Madison, WI, USA) was used to generate a standard curve.

## 2.10 | Measuring ecto-5'-nucleotidase activity

Ecto-5'-nucleotidase (NT5E, also known as CD73) activity was evaluated using the malachite green assay as previously described.<sup>43</sup> Briefly, 5  $\mu\text{g}$  of membrane proteins in 200  $\mu\text{L}$  of CD73 lysis buffer (10 mM Tris-HCl pH 7.5, 0.1% Nonidet P-40) was incubated at 37°C for 10 min, followed by incubation with 2 mM adenosine monophosphate (AMP) (Oriental Yeast Co., Ltd, Tokyo, Japan) at 37°C for 1 h. Next, 50  $\mu\text{L}$  of the reaction solution was mixed with 100  $\mu\text{L}$  of Biomol Green (Enzo Life Sciences, USA) and incubated for 5 min at room temperature. The amount of inorganic phosphate released from AMP was quantified by measuring the absorbance at 595 nm using a Synergy H1 Hybrid multi-mode microplate reader. A standard curve was generated using 0–200  $\mu\text{M}$   $\text{Na}_2\text{HPO}_4$  solutions dissolved in CD73 lysis buffer.

## 2.11 | Measuring ENPP activity

ENPP activity was evaluated as previously described.<sup>43</sup> Briefly, 3  $\mu\text{g}$  of membrane proteins was incubated with 100  $\mu\text{L}$  of 0.1 mM *p*-nitrophenyl thymidine 5-monophosphate (*p*NP-TMP; Sigma-Aldrich) solution at 37°C for 30 min. The *p*-nitrophenol released from *p*NP-TMP by ENPP1 and ENPP3 was quantified by measuring the absorbance at 405 nm. A standard curve was generated using human recombinant ENPP1 (R&D Systems, Minneapolis, MN).

## 2.12 | Inductively coupled plasma-mass spectrometry (ICP-MS) analysis

Zn, Mn, and Cu content was determined as previously described.<sup>47,50</sup> Briefly, cells were washed three times in PBS containing 1 mM EDTA and collected into a tall beaker with sterilized water. Samples were subsequently heated to 180°C, and 60% HNO<sub>3</sub>, 60% HClO<sub>4</sub>, and 30% H<sub>2</sub>O<sub>2</sub> were added. This procedure was repeated until all organic material was removed. Next, samples were cooled to room temperature, the residues were resuspended in 5 mL HNO<sub>3</sub> (5%) and sonicated with an ultrasonic bath sonicator for 30 s, and the solutions were used to quantify Zn, Mn, and Cu concentration via ICP-MS (Agilent 7700x and MassHunter; Agilent Technologies, Inc., Santa Clara, CA, USA). The tall beakers and sample cups used in this experiment were pretreated with 1% (v/v) HNO<sub>3</sub> to avoid metal contamination.

## 2.13 | Statistical analyses

Statistical analysis was performed using GraphPad Prism 9 (GraphPad Software; <https://www.graphpad.com/>). All data are expressed as the mean ± standard deviation (SD) from triplicate experiments. Statistical significance was determined using one-way ANOVA followed by Tukey's post hoc test *t*- at *p* < .05 and *p* < .01.

## 3 | RESULTS

### 3.1 | Mn treatment reduces the expression of Zn homeostatic proteins and Zn enzyme activity by causing Zn deficiency

To examine the effects of Mn on Zn metabolism, we first examined the expression changes in the Zn homeostatic proteins MT and ZNT1 in human near-haploid HAP1 cells cultured in the presence or absence of 20 μM MnSO<sub>4</sub>. Mn treatment (4 μM MnSO<sub>4</sub>) decreased the expression of Mn-sensitive protein TMEM165 and reduced MT and ZNT1 expression (Figure 1A left). Immunofluorescence staining showed that the same Mn treatment decreased cell surface ZNT1 expression in a dose-dependent manner (Figure 1B). The decreased expression of MT and ZNT1 was reminiscent of Zn deficiency in cells, according to our previous study.<sup>32</sup> Thus, we examined whether Mn treatment caused Zn deficiency in HAP1 cells. As expected, the activity of TNAP, a Zn-dependent enzyme,<sup>41-43</sup> decreased in a Mn concentration-dependent manner (Figure 1C left). ICP-MS analysis revealed that Mn treatment caused decreases in the cellular Zn content (Figure 1D). The effects

caused by Mn treatment were similar to those caused by Zn deficiency (CX in each panel in Figure 1A,C), where MT and ZNT1 expression (Figure 1A left) and TNAP activity (Figure 1C left) were substantially decreased. Zn supplementation almost completely reversed the effects of Mn treatment on MT and ZNT1 expression (Figure 1A right) and TNAP activity (Figure 1C right). Notably, Mn treatment used in these experiments had no toxic effects on the cells (Figure S1A). These results indicated that increased Mn content affects Zn homeostasis by reducing Zn content in cells.

Subsequently, we examined whether Cu treatment may cause effects similar to those of Mn treatment. We performed a set of experiments using the same concentrations of Cu as that of Mn (indicated above). MT and ZNT1 expression in HAP1 cells cultured in the presence or absence of Cu was not altered, as evident from the immunoblotting results (Figure 2A) and immunofluorescence analyses (Figure 2B). Moreover, TNAP activity (Figure 2C) and cellular Zn content were not altered by the Cu treatment, despite Cu content increasing (Figure 2D). The Cu treatment used in these experiments caused no toxic effects (Figure S1B).

### 3.2 | Alteration of cellular Mn homeostasis owing to the loss of Mn efflux protein affects Zn homeostasis

We examined the effect of Mn on Zn homeostasis in cells by modulating protein expression involved in cellular Mn homeostasis without treating the cells with high Mn concentrations. To this end, we established HAP1 cells deficient in *SPCA1* (HAP-*SPCA1*-KO cells, Table S1) since HAP1 cells only express the *SPCA1* mRNA of two important Mn efflux proteins, ZNT10 and *SPCA1*<sup>44,51-55</sup> (Figure S2A). Both MT and ZNT1 expression decreased in HAP-*SPCA1*-KO cells, along with decreased expression of TMEM165 (Figure 3A). Similarly, TNAP activity decreased in HAP-*SPCA1*-KO cells compared with that in WT HAP1 cells (Figure 3B). The observed defects in HAP-*SPCA1*-KO cells were restored by exogenous expression of ZNT10, a potent Mn efflux protein<sup>54,55</sup> (Figure 3A,B). Moreover, the decreased MT and ZNT1 expression in HAP-*SPCA1*-KO cells was rescued by Zn supplementation (up to 100 μM ZnSO<sub>4</sub>) (Figure 3C). The same Zn supplementation also restored TNAP activity (Figure 3D) and TMEM165 expression (in a dose-dependent manner; Figure 3C). These results suggest that Zn homeostasis would be affected by Mn, even without Mn supplementation, when Mn efflux activity is defective. Subsequently, we examined whether Zn treatment affected Mn content using HAP1 cells deficient in *ZNT1* (HAP-*ZNT1*-KO cells).<sup>32</sup> As expected, TMEM165 expression increased in HAP-*ZNT1*-KO

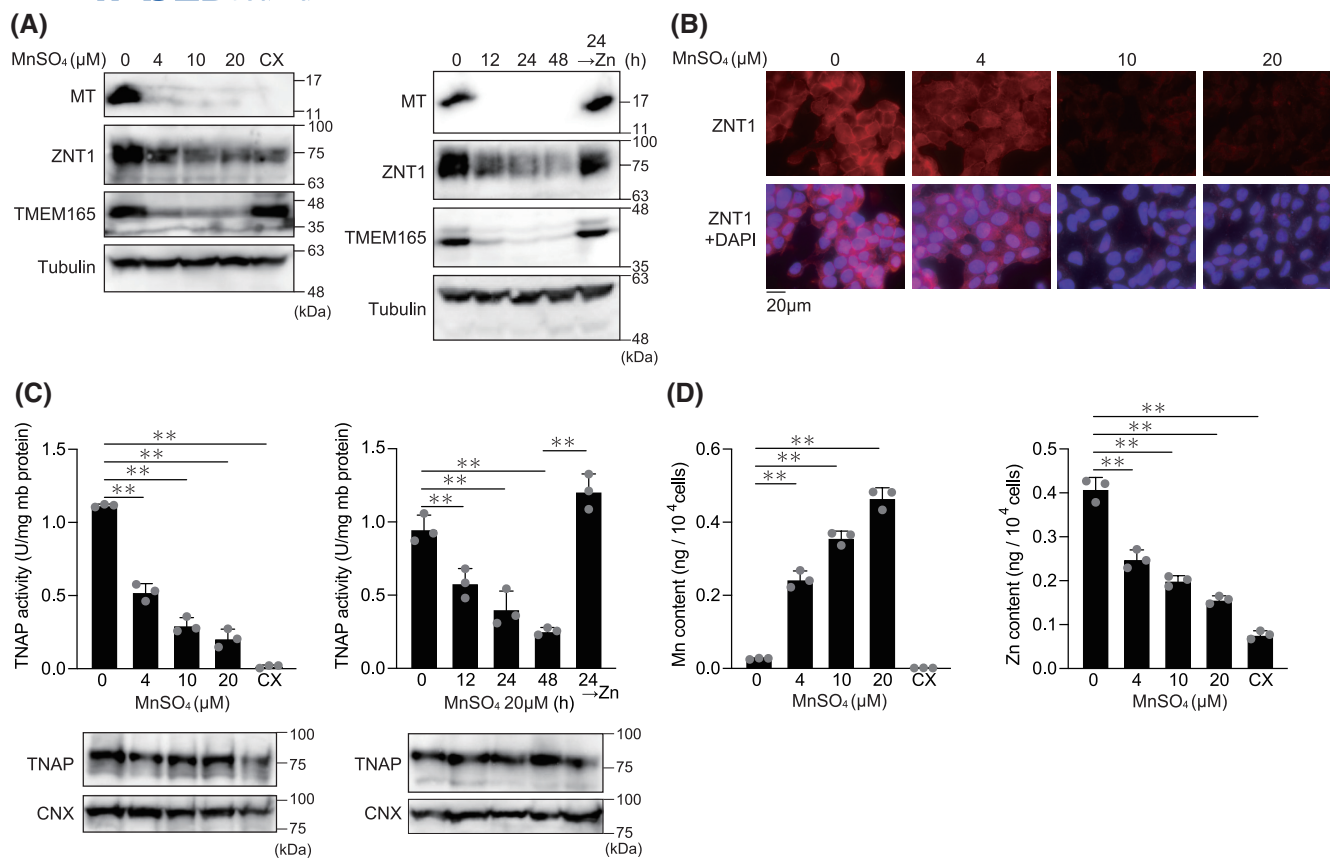


**FIGURE 1** Mn treatment reduced MT and ZNT1 expression as well as TNAP activity by decreasing Zn content in HAP1 cells. (A) Mn reduced MT and ZNT1 expression. Cells were cultured in a medium containing the indicated MnSO<sub>4</sub> concentration for 24 h (*left*) or cultured in a medium containing 20 μM MnSO<sub>4</sub> for the indicated period (*right*). CX: Zn-deficient medium, 24 → Zn: cultured in a medium containing 20 μM MnSO<sub>4</sub> for 24 h, then in 20 μM ZnSO<sub>4</sub> for 24 h. (B) Mn treatment reduced cell surface ZNT1 expression when cultured as in A (*left* panel). (C) Mn reduced TNAP activity in membrane fractions prepared from cells cultured as in A. U, unit. mb, membrane. (D) Mn decreased cellular Zn content. The cellular Zn and Mn contents were measured by ICP-MS. Statistical significance was determined using one-way ANOVA, followed by Tukey's post hoc test in panels C and D; \*\**p* < .01. Tubulin and calnexin (CNX) were used as loading controls in A and C. MT was detected using different PVDF membranes transferred from polyacrylamide gels of different percentages. Each experiment was performed at least three times, and representative results from independent experiments are shown.

cells and returned to the basal level following ZNT1 repression (Figure 3E). Increased TMEM165 expression was also suppressed by Mn supplementation (Figure 3F); thus, suggesting that cellular Mn content was affected by cellular Zn levels. Furthermore, we generated HAP1 cells deficient in both *ZNT1* and *SPCA1* (HAP-*ZNT1SPCA1*-DKO cells, Table S1) and examined the changes in MT and TMEM165 expression. MT expression was increased in HAP-*ZNT1SPCA1*-DKO cells, whereas TMEM165 expression was reduced in these cells (Figure 3G). These results suggest that both Zn and Mn contents increased in HAP-*ZNT1SPCA1*-DKO cells and that Zn and Mn homeostatic controls closely interact with each other.

We also investigated the interaction of Cu with Zn in HAP1 cells by establishing HAP1 cells deficient in *ATP7A* and/or *ATP7B* (HAP-*ATP7A*-KO, HAP-*ATP7B*-KO, and HAP-*ATP7A7B*-DKO cells, Table S1) because HAP1 cells

express both *ATP7A* and *ATP7B* as Cu efflux proteins (Figure 2B). MT and ZNT1 expression, as well as TNAP activity, was not decreased in all KO cells similar to that with Cu treatment (Figure 4A). However, MT expression substantially increased in cells lacking *ATP7A* (Figure 4B).<sup>29</sup> Thus, loss of *ATP7A* and/or *ATP7B* did not show Zn-deficient defects as those caused by the loss of *SPCA1* in HAP1 cells.

### 3.3 | Close interactions of Mn and Zn homeostasis in other human diploid cells

We investigated whether there are close interactions between Mn and Zn in other human diploid cells. We used the human hepatoma cell line HepG2 and human pancreatic cancer cell line PANC1 because the liver and pancreas are important organs for Mn and Zn metabolism.

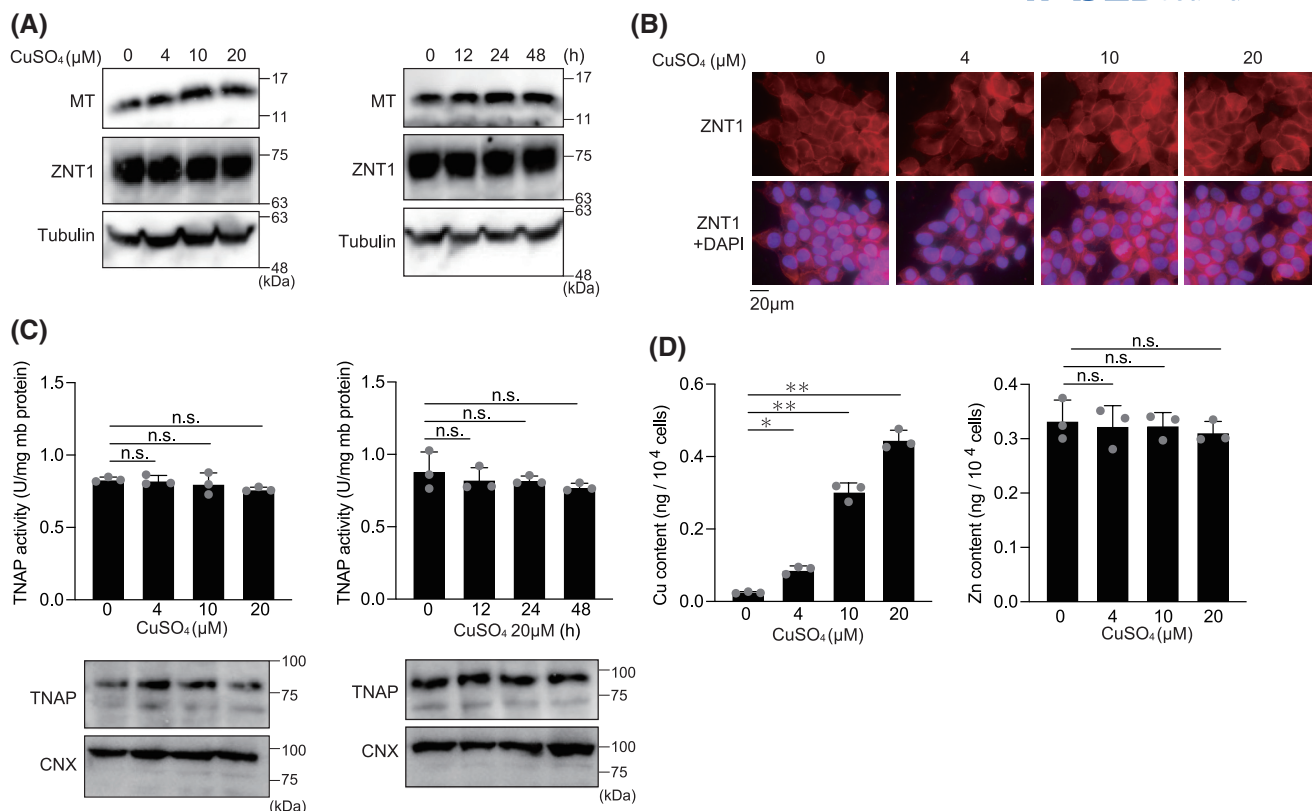


**FIGURE 2** Cu treatment did not alter MT and ZNT1 expression, the activity of TNAP, and the cellular Zn content in HAP1 cells. (A) MT and ZNT1 expression was not altered by Cu treatment. Cells were cultured in a medium containing the indicated CuSO<sub>4</sub> concentrations. The concentrations of CuSO<sub>4</sub> used were the same as those of MnSO<sub>4</sub> in Figure 1A. (B) Cu treatment did not reduce the surface ZNT1 expression in cells cultured as in A (left panel). (C) TNAP activity in membrane fractions was not altered by Cu treatment. U, unit. mb, membrane. (D) Cu treatment did not decrease cellular Zn content. The cellular Zn and Cu contents were measured using ICP-MS. Statistical significance was determined using one-way ANOVA, followed by Tukey's post hoc test in panels C and D; \*\* $p < .01$ ; \* $p < .05$ ; n.s., not significant. Tubulin and calnexin (CNX) were used as loading controls in A and C. MT was detected using the PVDF membranes transferred from polyacrylamide gels of different percentages. Each experiment was performed at least three times, and representative results from independent experiments are shown.

Metallothionein and ZNT1 expression, together with cell surface ZNT1 expression, decreased in a dose-dependent manner following Mn treatment of HepG2 cells (Figure 5A left and C) and PANC1 cells (Figure 5B left and D), similar to that observed in HAP1 cells. The decreased expression of TMEM165 induced by the Mn treatment was also observed in both cells. Furthermore, the activities of Zn-dependent enzymes ENPP1 and ENPP3 in HepG2 cells (Figure 5E) and CD73 in PANC1 cells decreased in the same culture conditions (Figure 5F). These enzymes were used because TNAP is not expressed in both cells.<sup>43</sup> As in the case of HAP1 cells, the decreased expression of MT and ZNT1 and the decreased enzyme activities were restored by the addition of Zn (20 μM ZnSO<sub>4</sub>) in HepG2 cells (Figure 5A right and E right) and PANC1 cells (Figure 5B right and F right). The Mn treatment had no apparent toxic effects on either cell type (Figure S1C,D).

An increase in the TMEM165 expression was observed in HepG2 cells (Figure 6A) and PANC1 cells

(Figure 6B) following the Zn treatment; thus, suggesting that the Mn content in both cells decreased, which was probably triggered by an increase in Zn levels. However, a minor change in TMEM165 expression was observed in HAP1 cells following the same Zn treatment (Figure 6C). Nevertheless, an increased TMEM165 expression was clearly observed in HAP-ZNT1-KO cells (Figure 3E), suggesting that this response is cell specific. Taken together, Zn and Mn metabolism closely interact with each other in human cells.

### 3.4 | ZIP8 oppositely regulates ZNT1 and MT expression depending on whether Zn or Mn is elevated in the extracellular milieu

Because ZIP8 and ZIP14 are known to transport extracellular Zn and Mn into cells,<sup>56–58</sup> they would be involved

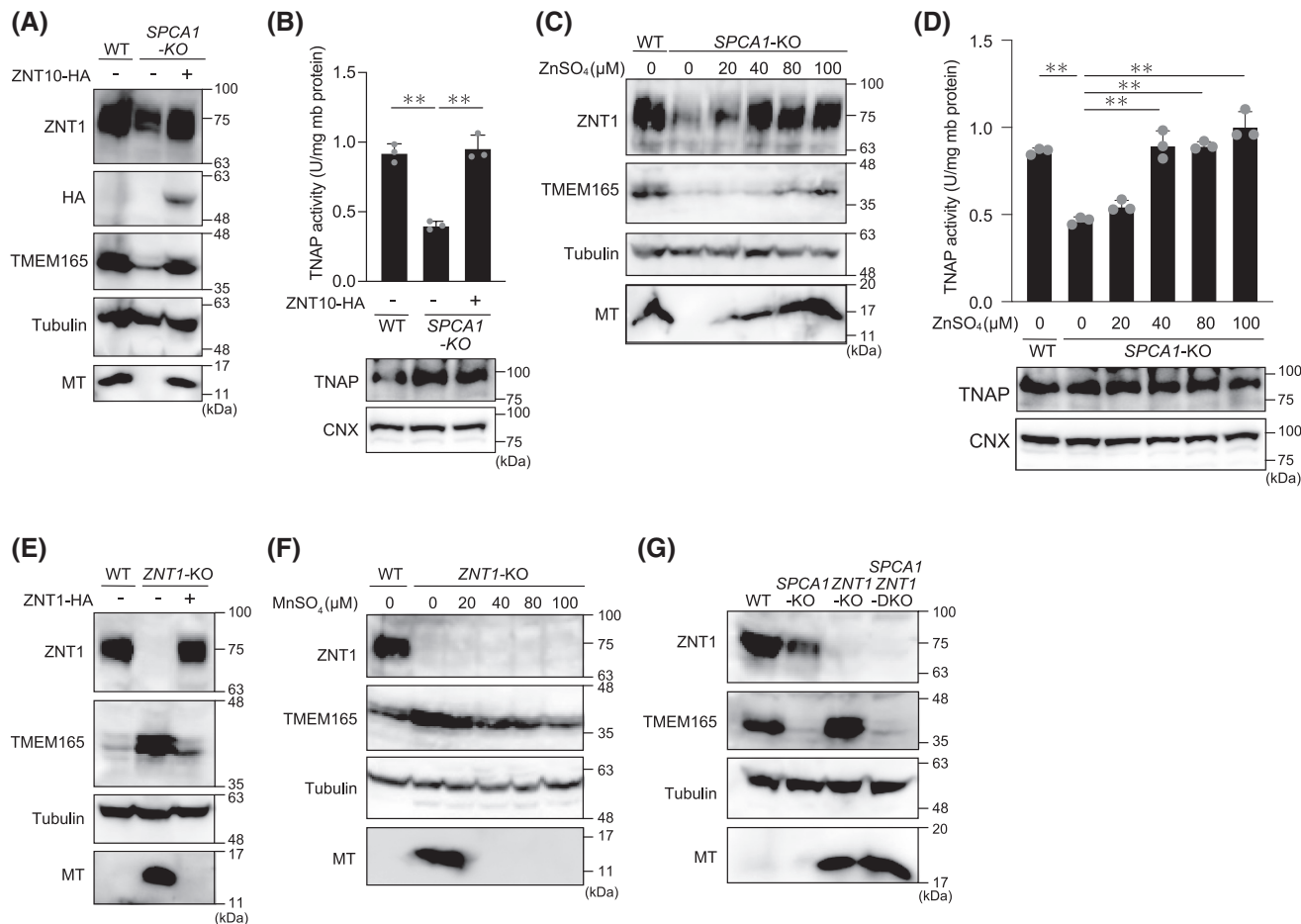


**FIGURE 3** Alteration of cellular Mn homeostasis caused by the loss of Mn efflux protein affects Zn homeostasis. (A) ZNT1 and MT expression was reduced in HAP-*SPCA1*-KO cells and was restored by expressing ZNT10-HA. (B) TNAP activity was reduced in HAP-*SPCA1*-KO cells and was restored by expressing ZNT10-HA. (C and D) The reduced expression of ZNT1 and MT (C), and the reduced activity of TNAP (D) in HAP-*SPCA1*-KO cells were reversed by supplementation of the indicated concentrations of ZnSO<sub>4</sub> for 24 h. (E) TMEM165 expression was increased in HAP1-*ZNT1*-KO cells, which was restored by expressing ZNT1-HA. (F) The increased expression of TMEM165 in HAP-*ZNT1*-KO cells was reversed by supplementation of the indicated concentrations of MnSO<sub>4</sub> for 24 h. (G) MT expression was increased, while TMEM165 expression was reduced in HAP-*ZNT1**SPCA1*-DKO cells. In A–G, tubulin and calnexin (CNX) were used as loading controls. MT was separated using polyacrylamide gels of different percentages. In B and D, statistical significance was determined using one-way ANOVA followed by Tukey's post hoc test; \*\**p* < .01. Each experiment was performed at least three times, and representative results from independent experiments are shown.

in the homeostatic interactions between Mn and Zn. We examined this possibility by analyzing MT and ZNT1 expression in cells overexpressing ZIP8. To perform this, we established MDCK cells (harboring FLP-In™ T-Rex) that stably express WT ZIP8 or a loss-of-function ZIP8 E343A mutant (Figure 7A,B), wherein an essential amino acid residue in the transmembranous Zn-binding site was substituted (343 Glu in the transmembrane helix V was substituted with Ala).<sup>59</sup> We used the cell system because it enabled the expression of WT ZIP8 and E343A ZIP8 mutant at almost the same levels under the control of the Tet-regulatable promoter (using doxycycline (Dox)); as a result, the transgene was integrated into the same locus by the FLP-In™ T-Rex system. Dox-induced ZIP8 expression increased MT and ZNT1 expression in

the normal culture medium (containing Zn derived from the FCS) (Figure 7A lane 5 vs. lane 1), which was triggered by Zn uptake (Figure 7C), whereas the addition of low Mn concentrations (up to 4 μM) decreased the ZIP8-induced expression of MT and ZNT1 to the basal level (which was the same level as that without Dox treatment). This was also accompanied by a reduction in TMEM165 expression. The reduction in MT, ZNT1, and TMEM165 expression was attributed to the decreased Zn content, which was owing to increases in Mn content (Figure 7C). These responses were not observed in the ZIP8 E343A null mutant (Figure 7B), owing to its loss of Zn and Mn transport ability (Figure 7C). Responses of MT and ZNT1 expression were consistent in MDCK cells stably expressing Zip14 (Figure S3A); however, this was not the case

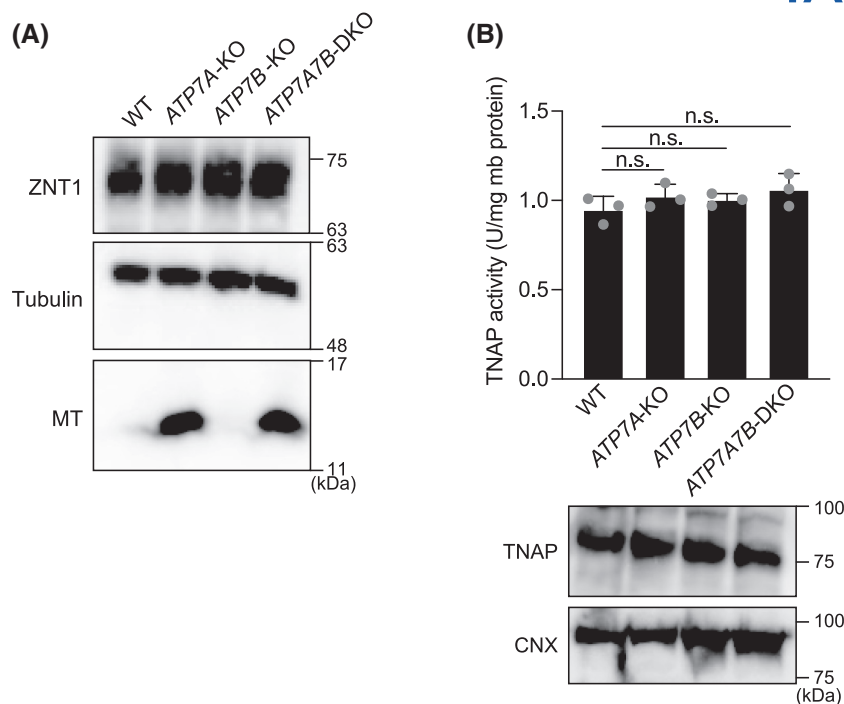


**FIGURE 4** Alteration of cellular Cu homeostasis caused by the loss of Cu efflux protein did not affect Zn homeostasis. (A) ZNT1 expression was not decreased in the indicated mutant HAP1 cells lacking Cu efflux proteins, whereas MT expression was increased in HAP-*ATP7A*-KO and HAP-*ATP7A7B*-DKO cells. (B) TNAP activity was not changed in the indicated mutant cells lacking Cu efflux proteins. In A and B, tubulin and calnexin (CNX) were used as loading controls. MT was detected using different PVDF membranes transferred from polyacrylamide gels of different percentages. In B, statistical significance was determined using one-way ANOVA followed by Tukey's post hoc test; n.s., not significant. Each experiment was performed at least three times, and representative results from independent experiments are shown.

in cells expressing a Zn-specific ZIP transporter such as ZIP5 (Figure S3B). These results indicate that cellular Zn homeostasis in cells expressing ZIP8 and/or ZIP14 is oppositely regulated depending on whether Zn or Mn levels are elevated in the extracellular space.

## 4 | DISCUSSION

Homeostatic interaction between Zn and Mn is less examined in mammals than in bacteria and yeast.<sup>60,61</sup> This study reports several important findings regarding the effects of Mn on Zn homeostasis, their close interactions, and changes in the expression of proteins involved in Mn and Zn homeostasis in mammalian cells. Mn and Zn compete in mammalian cells: excess Mn treatment or cells lacking Mn efflux protein (SPCA1) reduced the expression of Zn homeostatic proteins (MT and ZNT1) and Zn enzyme activities by decreasing Zn content. Notably, Zn homeostasis was not altered in cells treated with Cu at the same concentration or in cells lacking Cu efflux proteins (*ATP7A* and *ATP7B*). These lines of evidence provide novel insights into the homeostatic maintenance of systemic and cellular interaction of these trace elements.

Our results raise an important question of whether Mn and Zn compete in mammalian cells. Unfortunately, we do not have an answer to this question at present, although we have a hypothesis. Zn is known to bind to Asp, Glu, Asn, and Gln residues, in addition to preferentially binding to His and Cys residues,<sup>62–64</sup> whereas Mn preferentially binds to Asp, Glu, and Asn residues, in addition to the His residue.<sup>65</sup> These features have been shown in ZNT10 or ZIP14 and ZIP8; in the former case, the transmembranous Zn-binding motif HDHD that is conserved among ZNT family proteins is changed to NDHD (H: His, D: Asp, and N: Asn),<sup>55,66</sup> whereas, in the latter case, the semi-conserved His is changed to Glu in the transmembrane bi-nuclear metal center.<sup>69,67</sup> Thus, the competition between Zn and Mn may occur within proteins possessing these amino acid residues (Asp, Glu, and Asn) at Zn- or Mn-binding sites in the cells. If this is true, the competition between Zn and Mn would occur on proteins different from those involved in the competition between Zn and Cu because Zn and Cu competition is thought to occur on His and Cys residues in proteins,<sup>68</sup> such as MT (MT contains 20 Cys residues in approximately 60 amino acids). Mn does not bind to MT.<sup>69</sup> The result that the loss of Cu or Mn efflux proteins had opposite effects on MT

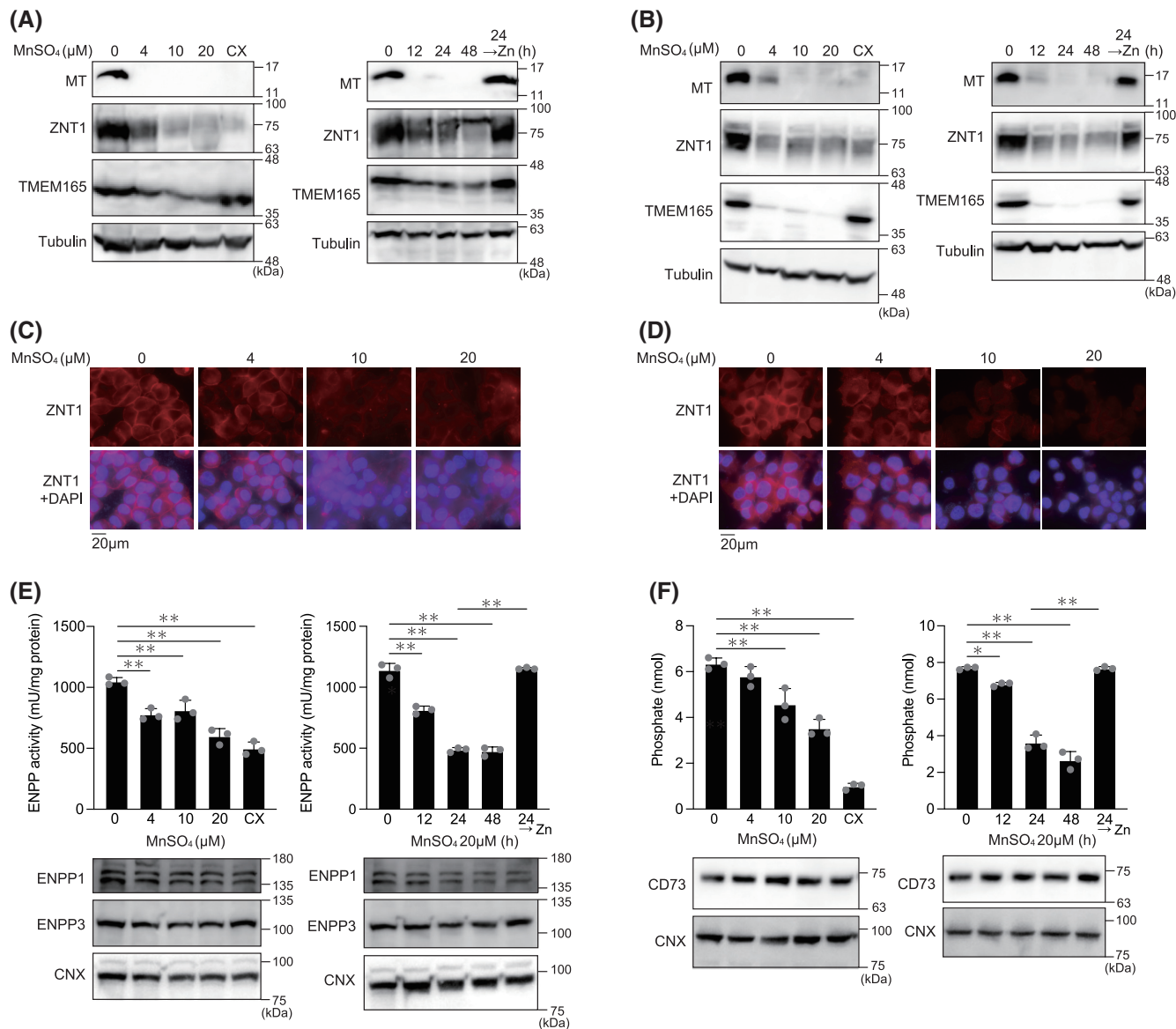


**FIGURE 5** Mn and Zn metabolism interacts in general cells. (A and B) Mn reduced MT and ZNT1 expression in HepG2 (A) and PANC1 cells (B). Cells were cultured under the same conditions as those described in Figure 1A. (C and D) Mn reduced cell surface ZNT1 expression. HepG2 (C) and PANC1 cells (D) were cultured in a medium containing the indicated MnSO<sub>4</sub> concentration for 24 h. (E and F) Mn reduced ENPP (ENPP1 and ENPP3) activity in HepG2 cells (E) and CD73 activity in PANC1 cells (F). ENPP or CD73 activity was measured using membrane proteins prepared from the respective cells cultured under the same conditions as those described in A and B. U, unit. mb, membrane. Statistical significance was determined using one-way ANOVA followed by Tukey's post hoc test in panels A, B, E, and F; \*\* $p < .01$ , \* $p < .05$ . Tubulin and calnexin (CNX) were used as loading controls in A, B, E, and F. MT was detected using different PVDF membranes transferred from polyacrylamide gels of different percentages. Each experiment was performed at least three times, and representative results from independent experiments are shown.

and ZNT1 expression provides evidence that the homeostasis of essential trace elements closely interacts with one another.

The increased Mn levels influenced MT and ZNT1 expression in HAP-SPCA1-KO cells under normal culture conditions without Mn supplementation. This result strongly suggests that decreased expression of Mn efflux proteins may affect cellular Zn homeostasis under physiological conditions. The decreased MT and ZNT1

expression would reflect homeostatic responses to minimize the decline in cytosolic Zn levels. This would be achieved by releasing Zn from MT due to degradation, and by inhibiting Zn efflux from cells via ZNT1 degradation because these homeostatic responses are observed during Zn deficiency.<sup>30–32</sup> Considering the time course of the changes in expression levels of the analyzed proteins, the alteration of MT expression was more rapid and sensitive to excess Mn than that of ZNT1 expression. Therefore, Zn

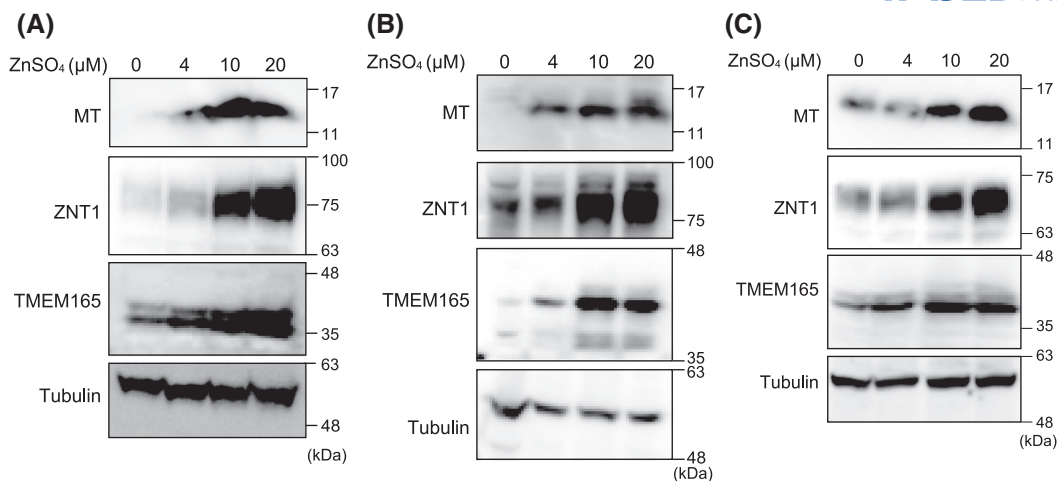


**FIGURE 6** Zn treatment increased TMEM165 expression. A-C. TMEM165 expression was increased in HepG2 (A), PANC1 (B), and HAP1 cells (C), cultured in a medium containing the indicated concentration of ZnSO<sub>4</sub> for 24 h. MT and ZNT1 were used as positive controls, and tubulin was used as a loading control. MT was detected using different PVDF membranes transferred from polyacrylamide gels of different percentages. Each experiment was performed at least three times, and representative results from independent experiments are shown.

homeostasis would be initially controlled by MT expression (through its degradation) and then by ZNT1 expression (by decreasing Zn efflux) to keep Zn levels within a homeostatic range in excess Mn situations.

MT expression decreased in HAP1-SPCA1-KO cells (Figure 3A), and TMEM165 expression increased in HAP1-ZNT1-KO cells (Figure 3E); thus, indicating that Zn content decreased in HAP1-SPCA1-KO cells, whereas Mn content decreased in HAP1-ZNT1-KO cells. In contrast, MT expression increased and TMEM165 expression decreased in HAP1-ZNT1SPCA1-DKO cells, indicating that both Zn and Mn contents were higher in HAP1-ZNT1SPCA1-DKO cells than those in WT HAP1 cells. This response may be simply explained by assuming that the regulatory mechanism to keep the ratio of Zn to Mn (and *vice versa*, which is inversely correlated) will not work if both Zn and Mn contents exceed their fixed upper limits. Alternatively, the upper limits of Zn and Mn content may be reset to higher levels than those in WT HAP1 cells when both Zn and Mn contents exceed the original limit operative in WT HAP1 cells. Although we have not determined which explanation best fits our findings, we would like to propose that ZNT1 and SPCA1 may function as master regulators of Zn and Mn sensing and buffering, at least in HAP1 cells.

Zn supplementation increased TMEM165 expression (to a certain extent) in all human cells examined in this study, probably by decreasing the Mn content, whereas Zn deficiency (represented by CX in Figure 1A right and Figure 5A,B right) did not decrease its expression. We assumed that this was because the Zn deficiency was not sufficient to increase Mn content, resulting in unresponsive TMEM165 expression. This suggests that there is a

low possibility that Zn deficiency directly disturbs Mn homeostasis. Nevertheless, this possibility should be further investigated.

The experiments in this study were performed using low concentrations of Mn (μM range), which may raise the question of whether such concentrations occur in our bodies. Human serum contains approximately 12–16 μM Zn<sup>70</sup> and 4.7–215 nM Mn,<sup>12,71</sup> and human plasma contains 551–925 μg/L Zn and 0.63–2.26 μg/L Mn,<sup>12,72</sup> indicating that the Mn content is much lower than the Zn content. Although we do not have data to verify the presence of low concentrations of Mn (μM range) in physiological conditions in the human body, we assume that the Mn concentration would reach close to the Zn concentration in certain situations. It is reported that Mn concentration in the bile can exceed that in the plasma by 100-fold,<sup>73</sup> and that Zn concentration is close to that in the plasma<sup>74</sup>; thus, suggesting that Zn and Mn concentrations may become close in the bile. If ZIP8 functions as an importer of Mn from the bile in the liver as proposed in previous studies,<sup>21,75</sup> ZIP8 may take up more Mn in hepatocytes than Zn as it has been shown to have a high affinity for Mn than Zn.<sup>76</sup> This hypothesis is likely because mutations of ZIP8/SLC39A8 result in systemic Mn deficiency, leading to reduced activity of Mn-dependent glycosyl transferases, and ultimately resulting in CDG.<sup>27,28</sup> Here, we showed that MT and ZNT1 expression was altered in MDCK cells overexpressing ZIP8 or Zip14 depending on whether Zn or Mn concentration is elevated in the extracellular space; however, this response was not observed in MDCK cells expressing ZIP5. This indicates that the cellular Zn homeostasis is unlikely to be changed in cells not expressing ZIP8 or ZIP14. This finding is important because cells

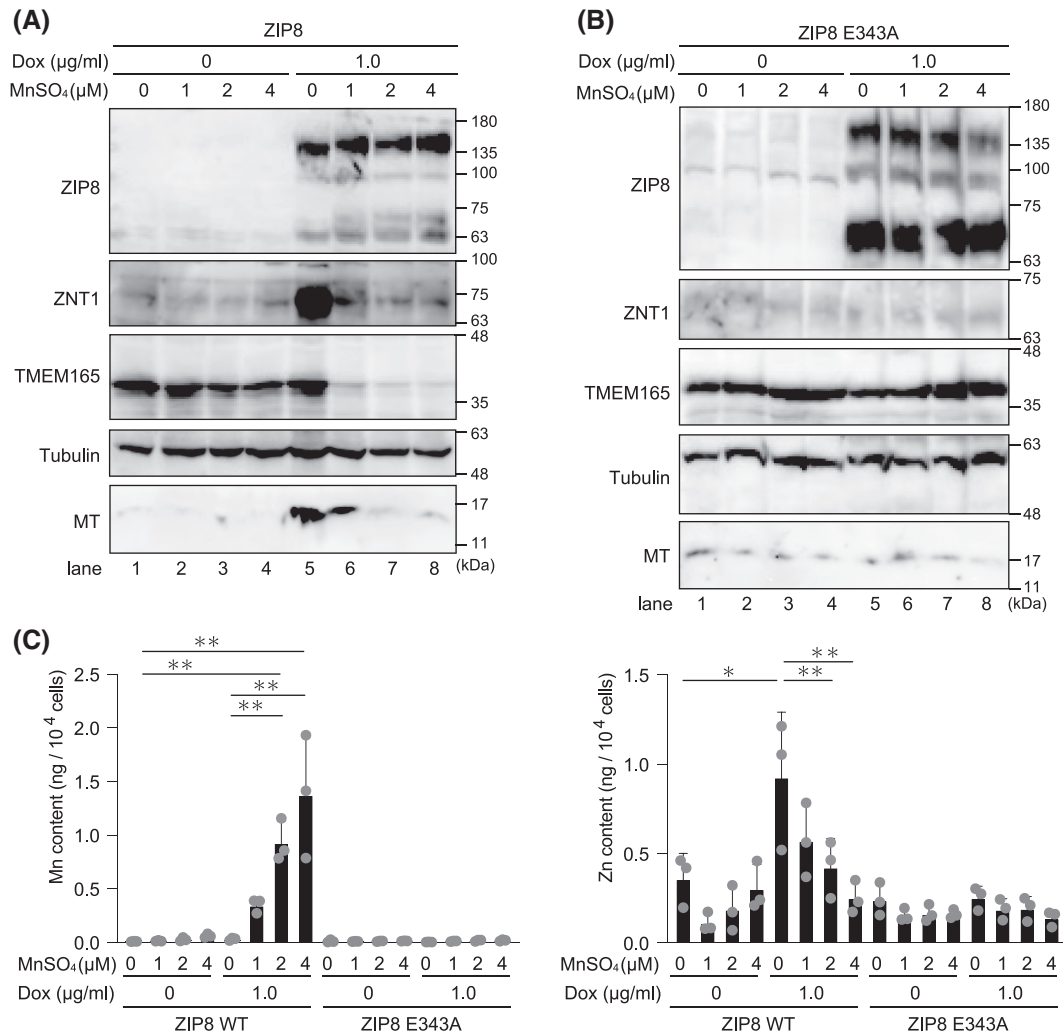


**FIGURE 7** Increased expression of ZIP8 oppositely regulates Zn homeostasis depending on whether Zn or Mn is elevated in the extracellular milieu. (A) Increased expression of ZNT1, MT, and TMEM165, which was triggered by Dox-induced expression of WT ZIP8, was reduced to the basal level in the presence of low concentrations of Mn. (B) Dox-induced expression of the loss-of-function ZIP8 E343A mutant had no effects on the expression of ZNT1, MT, and TMEM165. In A and B, MDCK cells stably expressing ZIP8 WT or ZIP8 E343A mutant were cultured with or without 1.0 μg/mL Dox for 24 h in the presence of the indicated MnSO<sub>4</sub> concentrations after culturing in medium supplemented with or without 1.0 μg/mL Dox for 4 h. Tubulin was used as a loading control. (C) Cellular Mn (left) or Zn (right) content in MDCK cells stably expressing the ZIP8 WT or ZIP8 E343A mutant cultured under the same conditions as those described in A and B. Cellular Mn or Zn content was measured using ICP-MS. In C, statistical significance was determined using one-way ANOVA followed by Tukey's post hoc test. \*\* $p < .01$ , \* $p < .05$ . Each experiment was performed at least three times, and representative results from independent experiments are shown.

always have to adapt to changes in Zn and Mn in the extracellular milieu. A detailed kinetic study is required to clarify the effects of Mn uptake mediated by ZIP8 or ZIP14 on the alteration of Zn homeostasis in the future.

In conclusion, our results reveal that intracellular Mn and Zn homeostasis is intricately connected in mammalian cells. Moreover, we showed that homeostatic interactions between Zn and Mn likely occur in cells expressing ZIP8 or ZIP14 under certain circumstances. This information would facilitate our understanding of Mn physiopathology. The understanding of Mn as an essential micronutrient and a toxic trace element should continue

to progress since it may aid in the development of treatment strategies for Mn-related diseases.

#### AUTHOR CONTRIBUTIONS

Yukina Nishito and Taiho Kambe conceived the study and designed the experiments. Yukina Nishito, Yoshiaki Kamimura, Shino Nagamatsu, Nao Yamamoto, Hiroyuki Yasui, and Taiho Kambe collected, analyzed, and interpreted the data. Yukina Nishito prepared figures. Yukina Nishito and Taiho Kambe drafted the manuscript. Taiho Kambe edited the manuscript. All authors reviewed the manuscript.

## ACKNOWLEDGMENTS

We thank Taiki Komori and Namino Ogawa for their technical assistance. This work was supported by a Grant-in-aid for Scientific Research on Innovative Areas “Integrated Bio-metal Science” (MEXT KAKENHI Grant Number JP19H05768) from the Ministry of Education, Culture, Sports, Science, and Technology, Japan; a Grant-in-Aid for Scientific Research (B) (JSPS KAKENHI Grant Numbers JP19H02883 and JP22H02257) from the Japan Society for the Promotion of Science, the Sugiyama Chemical & Industrial Laboratory, the Kieikai Research Foundation, the Tojuro Iijima Foundation for Food Science and Technology, the KOSÉ Cosmetology Research Foundation, and The Naito Foundation (to T.K.); and a Grant-in-Aid for Young Scientists (JSPS KAKENHI Grant Number JP21K15262) from the Japan Society for the Promotion of Science (to Y.N.).

## DISCLOSURES

No conflicts of interest, financial or otherwise, are declared by the authors.

## DATA AVAILABILITY STATEMENT

All data generated or analyzed during this study are included in this published article (and its Supporting Information file) or are available from the corresponding author (Taiho Kambe, Kyoto University, Email: [kambe.taiho.7z@kyoto-u.ac.jp](mailto:kambe.taiho.7z@kyoto-u.ac.jp)) upon reasonable request. Full-length immunoblots corresponding to images in the main text and the supplementary figure are shown in [Figures S4–S12](#).

## ORCID

Hiroyuki Yasui  <https://orcid.org/0000-0003-3317-3947>

Taiho Kambe  <https://orcid.org/0000-0001-9757-063X>

## REFERENCES

- Beutler E, Hoffbrand AV, Cook JD. Iron deficiency and overload. *Hematology Am Soc Hematol Educ Program*. 2003;2003:40-61.
- Koch KA, Peña MM, Thiele DJ. Copper-binding motifs in catalysis, transport, detoxification and signaling. *Chem Biol*. 1997;4:549-560.
- Hambidge M. Human zinc deficiency. *J Nutr*. 2000;130:1344S-1349S.
- Aschner JL, Aschner M. Nutritional aspects of manganese homeostasis. *Mol Asp Med*. 2005;26:353-362.
- Wood RJ. Manganese and birth outcome. *Nutr Rev*. 2009;67:416-420.
- Aschner M, Erikson KM, Herrero Hernández E, Tjalkens R. Manganese and its role in Parkinson's disease: from transport to neuropathology. *NeuroMolecular Med*. 2009;11:252-266.
- Lucchini RG, Martin CJ, Doney BC. From manganism to manganese-induced parkinsonism: a conceptual model based on the evolution of exposure. *NeuroMolecular Med*. 2009;11:311-321.
- Kambe T, Weaver BP, Andrews GK. The genetics of essential metal homeostasis during development. *Genesis*. 2008;46:214-228.
- Sheqwarra J, Alkhatib Y. Sideroblastic anemia secondary to zinc toxicity. *Blood*. 2013;122:311.
- Hoffman HN 2nd, Phyllyk RL, Fleming CR. Zinc-induced copper deficiency. *Gastroenterology*. 1988;94:508-512.
- Collins JF, Prohaska JR, Knutson MD. Metabolic crossroads of iron and copper. *Nutr Rev*. 2010;68:133-147.
- Baj J, Flieger W, Barbachowska A, et al. Consequences of disturbing manganese homeostasis. *Int J Mol Sci*. 2023;24:14959.
- Brna P, Gordon K, Dooley JM, Price V. Manganese toxicity in a child with iron deficiency and polycythemia. *J Child Neurol*. 2011;26:891-894.
- Seo YA, Li Y, Wessling-Resnick M. Iron depletion increases manganese uptake and potentiates apoptosis through ER stress. *Neurotoxicology*. 2013;38:67-73.
- Seo YA, Elkhader JA, Wessling-Resnick M. Distribution of manganese and other biometals in flatiron mice. *Biometals*. 2016;29:147-155.
- Bowman AB, Kwakye GF, Herrero Hernández E, Aschner M. Role of manganese in neurodegenerative diseases. *J Trace Elem Med Biol*. 2011;25:191-203.
- Roth J, Ponzoni S, Aschner M. Manganese homeostasis and transport. *Met Ions Life Sci*. 2013;12:169-201.
- Fujishiro H, Kambe T. Manganese transport in mammals by zinc transporter family proteins, ZNT and ZIP. *J Pharmacol Sci*. 2022;148:125-133.
- Mukhopadhyay S, Linstedt AD. Identification of a gain-of-function mutation in a Golgi P-type ATPase that enhances Mn<sup>2+</sup> efflux and protects against toxicity. *Proc Natl Acad Sci USA*. 2011;108:858-863.
- Leitch S, Feng M, Muend S, Braiterman LT, Hubbard AL, Rao R. Vesicular distribution of secretory pathway Ca<sup>2+</sup>-ATPase isoform 1 and a role in manganese detoxification in liver-derived polarized cells. *Biometals*. 2011;24:159-170.
- Liu Q, Barker S, Knutson MD. Iron and manganese transport in mammalian systems. *Biochim Biophys Acta, Mol Cell Res*. 2021;1868:118890.
- Mukhopadhyay S. Familial manganese-induced neurotoxicity due to mutations in *SLC30A10* or *SLC39A14*. *Neurotoxicology*. 2018;64:278-283.
- Winslow JWW, Limesand KH, Zhao N. The Functions of ZIP8, ZIP14, and ZnT10 in the regulation of systemic manganese homeostasis. *Int J Mol Sci*. 2020;21:3304.
- Quadri M, Federico A, Zhao T, et al. Mutations in *SLC30A10* cause parkinsonism and dystonia with hypermanganesemia, polycythemia, and chronic liver disease. *Am J Hum Genet*. 2012;90:467-477.
- Tuschl K, Clayton PT, Gospe SMJ, et al. Syndrome of hepatic cirrhosis, dystonia, polycythemia, and hypermanganesemia caused by mutations in *SLC30A10*, a manganese transporter in man. *Am J Hum Genet*. 2012;90:457-466.
- Tuschl K, Meyer E, Valdivia LE, et al. Mutations in *SLC39A14* disrupt manganese homeostasis and cause childhood-onset parkinsonism-dystonia. *Nat Commun*. 2016;7:11601.
- Boycott KM, Beaulieu CL, Kernohan KD, et al. Autosomal-recessive intellectual disability with cerebellar atrophy syndrome caused by mutation of the manganese and zinc transporter gene *SLC39A8*. *Am J Hum Genet*. 2015;97:886-893.

28. Park JH, Hogrebe M, Grüneberg M, et al. SLC39A8 deficiency: a disorder of manganese transport and glycosylation. *Am J Hum Genet.* 2015;97:894-903.
29. Krężel A, Maret W. The functions of metamorphic metallothioneins in zinc and copper metabolism. *Int J Mol Sci.* 2017;18:1237.
30. Palmiter RD, Findley SD. Cloning and functional characterization of a mammalian zinc transporter that confers resistance to zinc. *EMBO J.* 1995;14:639-649.
31. Palmiter RD. Protection against zinc toxicity by metallothionein and zinc transporter 1. *Proc Natl Acad Sci USA.* 2004;101:4918-4923.
32. Nishito Y, Kambe T. Zinc transporter 1 (ZNT1) expression on the cell surface is elaborately controlled by cellular zinc levels. *J Biol Chem.* 2019;294:15686-15697.
33. McMahan RJ, Cousins RJ. Regulation of the zinc transporter ZnT-1 by dietary zinc. *Proc Natl Acad Sci USA.* 1998;95:4841-4846.
34. Langmade SJ, Ravindra R, Daniels PJ, Andrews GK. The transcription factor MTF-1 mediates metal regulation of the mouse ZnT1 gene. *J Biol Chem.* 2000;275:34803-34809.
35. Kimura T, Kambe T. The functions of metallothionein and ZIP and ZnT transporters: an Overview and perspective. *Int J Mol Sci.* 2016;17:336.
36. Kambe T, Tsuji T, Hashimoto A, Itsumura N. The physiological, biochemical, and molecular roles of zinc transporters in zinc homeostasis and metabolism. *Physiol Rev.* 2015;95:749-784.
37. Kambe T, Taylor KM, Fu D. Zinc transporters and their functional integration in mammalian cells. *J Biol Chem.* 2021;296:100320.
38. Drozd A, Wojewska D, Peris-Díaz MD, Jakimowicz P, Krężel A. Crosstalk of the structural and zinc buffering properties of mammalian metallothionein-2. *Metallomics.* 2018;10:595-613.
39. Krężel A, Maret W. The bioinorganic chemistry of mammalian metallothioneins. *Chem Rev.* 2021;121:14594-14648.
40. Lichten LA, Cousins RJ. Mammalian zinc transporters: nutritional and physiologic regulation. *Annu Rev Nutr.* 2009;29:153-176.
41. Suzuki E, Ogawa N, Takeda TA, et al. Detailed analyses of the crucial functions of Zn transporter proteins in alkaline phosphatase activation. *J Biol Chem.* 2020;295(17):5669-5684.
42. Ueda S, Manabe Y, Kubo N, et al. Early secretory pathway-resident Zn transporter proteins contribute to cellular sphingolipid metabolism through activation of sphingomyelin phosphodiesterase 1. *Am J Physiol Cell Physiol.* 2022;322:C948-C959.
43. Takeda TA, Miyazaki S, Kobayashi M, et al. Zinc deficiency causes delayed ATP clearance and adenosine generation in rats and cell culture models. *Commun Biol.* 2018;1:113.
44. Lebredonchel E, Houdou M, Hoffmann HH, et al. Investigating the functional link between TMEM165 and SPCA1. *Biochem J.* 2019;476:3281-3293.
45. Potelle S, Dulary E, Climer L, et al. Manganese-induced turnover of TMEM165. *Biochem J.* 2017;474:1481-1493.
46. Kambe T, Andrews GK. Novel proteolytic processing of the ectodomain of the zinc transporter ZIP4 (SLC39A4) during zinc deficiency is inhibited by acrodermatitis enteropathica mutations. *Mol Cell Biol.* 2009;29:129-139.
47. Nagamatsu S, Nishito Y, Yuasa H, et al. Sophisticated expression responses of ZNT1 and MT in response to changes in the expression of ZIPs. *Sci Rep.* 2022;12:7334.
48. Wagatsuma T, Suzuki E, Shiotsu M, et al. Pigmentation and TYRP1 expression are mediated by zinc through the early secretory pathway-resident ZNT proteins. *Commun Biol.* 2023;6:403.
49. Guttman S, Nadzemova O, Grünwald I, et al. ATP7B knockout disturbs copper and lipid metabolism in Caco-2 cells. *PLoS One.* 2020;15:e0230025.
50. Naito Y, Yoshikawa Y, Masuda K, Yasui H. Bis(hinokitiolato) zinc complex ([Zn(hkt)<sub>2</sub>]) activates Akt/protein kinase B independent of insulin signal transduction. *J Biol Inorg Chem.* 2016;21:537-548.
51. Leyva-Illades D, Chen P, Zogzas CE, et al. SLC30A10 is a cell surface-localized manganese efflux transporter, and parkinsonism-causing mutations block its intracellular trafficking and efflux activity. *J Neurosci.* 2014;34:14079-14095.
52. Taylor CA, Hutchens S, Liu C, et al. SLC30A10 transporter in the digestive system regulates brain manganese under basal conditions while brain SLC30A10 protects against neurotoxicity. *J Biol Chem.* 2019;294:1860-1876.
53. Xia Z, Wei J, Li Y, et al. Zebrafish slc30a10 deficiency revealed a novel compensatory mechanism of Atp2c1 in maintaining manganese homeostasis. *PLoS Genet.* 2017;13:e1006892.
54. Mercadante CJ, Prajapati M, Conboy HL, et al. Manganese transporter Slc30a10 controls physiological manganese excretion and toxicity. *J Clin Invest.* 2019;129:5442-5461.
55. Nishito Y, Tsuji N, Fujishiro H, et al. Direct Comparison of manganese detoxification/efflux proteins and molecular characterization of ZnT10 protein as a manganese transporter. *J Biol Chem.* 2016;291:14773-14787.
56. Aydemir TB, Cousins RJ. The multiple faces of the metal transporter ZIP14 (SLC39A14). *J Nutr.* 2018;148:174-184.
57. Jenkitkasemwong S, Wang CY, Mackenzie B, Knutson MD. Physiologic implications of metal-ion transport by ZIP14 and ZIP8. *Biomaterials.* 2012;25:643-655.
58. Nebert DW, Gálvez-Peralta M, Hay EB, et al. ZIP14 and ZIP8 zinc/bicarbonate symporters in *Xenopus* oocytes: characterization of metal uptake and inhibition. *Metallomics.* 2012;4:1218-1225.
59. Fujishiro H, Miyamoto S, Sumi D, Kambe T, Himeno S. Effects of individual amino acid mutations of zinc transporter ZIP8 on manganese- and cadmium-transporting activity. *Biochem Biophys Res Commun.* 2022;616:26-32.
60. Jacobsen FE, Kazmierczak KM, Lisher JP, Winkler ME, Giedroc DP. Interplay between manganese and zinc homeostasis in the human pathogen *Streptococcus pneumoniae*. *Metallomics.* 2011;3:38-41.
61. McDevitt CA, Ogguniyi AD, Valkov E, et al. A molecular mechanism for bacterial susceptibility to zinc. *PLoS Pathog.* 2011;7:e1002357.
62. Sousa SF, Lopes AB, Fernandes PA, Ramos MJ. The Zinc proteome: a tale of stability and functionality. *Dalton Trans.* 2009;7946-7956.
63. Permyakov EA. Metal binding proteins. *Encyclopedia.* 2021;1:261-292.
64. Auld DS. Zinc coordination sphere in biochemical zinc sites. *Biomaterials.* 2001;14:271-313.
65. Udayalaxmi S, Mohan RG, Ravikiran K, Ettaiah P. Investigation of manganese metal coordination in proteins: a comprehensive

- PDB analysis and quantum mechanical study. *Struct Chem*. 2020;31:1057-1064.
66. Kambe T, Suzuki E, Komori T. Zinc transporter proteins: a review and a new view from biochemistry. *Zinc Signaling*. Springer; 2019. 23 p.
67. Taylor KM, Nicholson RI. The LZT proteins; the LIV-1 subfamily of zinc transporters. *Biochim Biophys Acta*. 2003;1611:16-30.
68. Brylinski M, Skolnick J. FINDSITE-metal: integrating evolutionary information and machine learning for structure-based metal-binding site prediction at the proteome level. *Proteins*. 2011;79:735-751.
69. Waalkes MP, Harvey MJ, Klaassen CD. Relative in vitro affinity of hepatic metallothionein for metals. *Toxicol Lett*. 1984;20:33-39.
70. Maares M, Haase H. A guide to human zinc absorption: general overview and recent advances of in vitro intestinal models. *Nutrients*. 2020;12:762.
71. Chavan S, Bhat R, Nandoskar A, et al. Determination of manganese in serum using GFAAS: serum reference values for manganese in the adolescent girls of the DERVAN cohort. *Indian J Clin Biochem*. 2022;37:487-493.
72. Goullé JP, Mahieu L, Castermant J, et al. Metal and metalloid multi-elementary ICP-MS validation in whole blood, plasma, urine and hair. Reference values. *Forensic Sci Int*. 2005;153:39-44.
73. Klaassen CD. Biliary excretion of manganese in rats, rabbits, and dogs. *Toxicol Appl Pharmacol*. 1974;29:458-468.
74. Walsh CT, Sandstead HH, Prasad AS, Newberne PM, Fraker PJ. Zinc: health effects and research priorities for the 1990s. *Environ Health Perspect*. 1994;102:5-46.
75. Lin W, Vann DR, Doulias PT, et al. Hepatic metal ion transporter ZIP8 regulates manganese homeostasis and manganese-dependent enzyme activity. *J Clin Invest*. 2017;127:2407-2417.
76. He L, Girijashanker K, Dalton TP, et al. ZIP8, member of the solute-carrier-39. (SLC39) metal-transporter family: characterization of transporter properties. *Mol Pharmacol*. 2006;70:171-180.

## SUPPORTING INFORMATION

Additional supporting information can be found online in the Supporting Information section at the end of this article.

**How to cite this article:** Nishito Y, Kamimura Y, Nagamatsu S, Yamamoto N, Yasui H, Kambe T. Zinc and manganese homeostasis closely interact in mammalian cells. *The FASEB Journal*. 2024;38:e23605. doi:[10.1096/fj.202400181R](https://doi.org/10.1096/fj.202400181R)